The Chemistry of *N*-Alkylporphyrin Complexes: A Comparison of Reactivities and Structures of Chlorozinc(II) Complexes of *N*-Benzyl-, *N*-Methyl-, and *N*-Phenyltetraphenylporphyrin

Cynthia K. Schauer,[†] Oren P. Anderson,*[†] David K. Lavallee,*[‡] Jean-Paul Battioni,[§] and Daniel Mansuy[§]

Contribution from the Department of Chemistry, Colorado State University, Fort Collins, Colorado 80523, Department of Chemistry, Hunter College of the City University of New York, New York, New York 10021, and Laboratoire de Chimie et Biochimie Pharmacologiques et Toxicologiques, Université René Descartes, 75270 Paris Cédex 06, France.
Received September 11, 1986

Abstract: Zinc and copper complexes of N-substituted porphyrins undergo nucleophilic displacement of the N-substituent at rates that are strongly dependent on the nature of the N-substituent. Substituents capable of stabilizing incipient carbocations allow faster reaction. For the reactions of chloro(*N*-benzyltetraphenylporphinato)- and chloro(*N*-methyltetraphenylporphinato)zinc(II) complexes with di-*n*-butylamine, $\Delta H^{\ddagger}$ = 71 kJ mol^{-1}, $\Delta S^{\ddagger}$ = -92 J mol^{-1} K^{-1}, and $\Delta G^{\ddagger}$ = 100 kJ mol^{-1} (318 K) and $\Delta H^{\ddagger}$ = 176 kJ mol^{-1}, $\Delta S^{\ddagger}$ = 230 J mol^{-1} K^{-1}, and $\Delta G^{\ddagger}$ = 103 kJ mol^{-1} (318 K), respectively. The reaction of the chloro(*N*-phenyltetraphenylporphinato)zinc(II) complex is very slow. The structures of the *N*-benzyl and *N*-phenyl zinc(II) complexes have been determined by single-crystal X-ray diffraction ([Zn(*N*-Bz-TPP)Cl]: triclinic, a = 10.579 (2) Å, b = 12.310 (2) Å, c = 17.957 (3) Å, α = 85.31 (1)°, β = 80.89 (1)°, γ = 72.63 (1)°, -130 °C, $P\bar{1}$, Z = 2. [Zn(*N*-Ph-TPP)Cl]: orthorhombic, a = 15.078 (5) Å, b = 15.272 (5) Å, c = 17.268 (5) Å, 20 °C, $P2_12_12_1$, Z = 4). In each case, the coordination geometry is a highly distorted square pyramid, with chloride ion occupying the apical position and a long bond to the substituted nitrogen atom ([Zn(*N*-Bz-TPP)Cl], Zn-N1 = 2.477 (3) Å; [Zn(*N*-Ph-TPP)Cl], Zn-N1 = 2.492 (6) Å). The *N*-benzyl Zn(II) complex resembles the [Zn(TPP)] product of the displacement reaction more closely than does the *N*-methyl or the *N*-phenyl complex (Zn(II) displacement above the N2, N3, N4 reference plane of 0.67, 0.65, and 0.59 Å, cant of the N-substituted pyrrole ring from the reference plane of 42°, 39°, and 32°, and Zn-Cl bond distances of 2.227 (2), 2.232 (3), and 2.265 (1) Å for *N*-Ph, *N*-Me, and *N*-Bz, respectively). These structural changes are correlated with the relative rates of the nucleophilic displacement reactions for these complexes.

N-Substituted porphyrins have been identified as products from the interaction of drugs with cytochrome P-450 in animal liver and from reactions of aryl- and alkylhydrazines with hemoglobin.[1] Such porphyrins have typically been converted to zinc complexes for spectroscopic characterization.[2] Zinc complexes of *N*-alkylporphyrins have also been shown to be inhibitors of ferrochelatase and heme oxygenase, with the inhibition activity related to the nature of the N-substituent.[3] Recently, we have studied the effect of varying the N-substituent on the rate of nucleophilic displacement of that substituent from the N-substituted metalloporphyrin.[4] The effect of changing the N-substituent in copper(II) complexes is dramatic; *N*-benzylporphyrin complexes are more reactive (by several orders of magnitude) than are *N*-alkylporphyrin complexes, which are in turn more reactive than *N*-phenylporphyrin complexes. Because of the high reactivities of copper(II) complexes, we have not obtained suitable single crystals for structural comparisons among members of this series of complexes. Previously, we published the structural parameters for chloro(*N*-methyltetraphenylporphinato)zinc(II)[5] (hereafter [Zn(*N*-Me-TPP)Cl]), as well as a preliminary report of the structure of chloro(*N*-phenyltetraphenylporphinato)zinc(II) (hereafter [Zn(*N*-Ph-TPP)Cl]).[6] We now present a complete structural report for chloro(*N*-benzyltetraphenylporphinato)-zinc(II) (hereafter [Zn(*N*-Bz-TPP)Cl]) and for [Zn(*N*-Ph-TPP)Cl], together with kinetic results for the nucleophilic displacement of the *N*-benzyl substituent. The *N*-benzylporphyrin ligand was made by a new technique that allows the synthesis of a variety of *N*-benzylporphyrins in a single step of high yield (>90%). Comparison of the structural and kinetic results for the *N*-Bz-TPP complex with corresponding results for the *N*-Me and *N*-Ph complexes should allow us to see whether a correlation exists between the ground-state structures of these complexes and their reactivities with respect to displacement of the *N*-substituent.

Experimental Section

Synthesis of Complexes. To synthesize the *N*-benzyltetraphenylporphyrin ligand,[7] diphenylsulfonium tetrafluoroborate[8] was added in 10% excess to tetraphenylporphyrin (prepared by the method of Adler[9]) in dichloromethane. This mixture was either stirred overnight at room temperature or heated for 2 h at 120 °C in a Teflon-glass pressure vessel.[10] The resultant solution was neutralized with excess 1 M aqueous ammonia. The product was extracted with water and purified by column chromatography over neutral alumina with dichloromethane as eluant. The yield is typically greater than 90%.

[Zn(*N*-Bz-TPP)Cl] was synthesized by using a twofold excess of zinc chloride hydrate in acetonitrile. Repeated crystallization of the product from a mixture of dichloromethane and acetonitrile provided crystals suitable for the X-ray structure determination. These dark purple crystals were kept in mother liquor up to the time of the crystallographic experiment to prevent loss of occluded solvent. UV-visible spectrum: 439, 449, 560, 612, and 659 nm. Analysis was satisfactory for C, H, N, and Cl.

[†] Colorado State University.
[‡] Hunter College.
[§] Université René Descartes.

(1) (a) Ortiz de Montellano, P. R.; Correia, M. A. *Annu. Rev. Pharmacol. Toxicol.* **1983**, *23*, 481. (b) Mansuy, D.; Battioni, P.; Mahy, J.-P.; Gillet, G. *Biochem. Biophys. Res. Commun.* **1982**, *106*, 30. (c) Ortiz de Montellano, P. R.; Kunze, K. L. *J. Am. Chem. Soc.* **1982**, *105*, 1380. (d) Ringe, D.; Petsko, G. A.; Kerr, D. E.; Ortiz de Montellano, P. R. *Biochemistry* **1984**, *23*, 2.
(2) For example: Ortiz de Montellano, P. R.; Kunze, K. L. *J. Am. Chem. Soc.* **1981**, *103*, 4225.
(3) De Matteis, F. D.; Gibbs, A. H.; Harvey, C. *Biochem. J.* **1985**, *226*, 537.
(4) Lavallee, D. K.; Kuila, D. *Inorg. Chem.* **1984**, *23*, 3987.
(5) Lavallee, D. K.; Kopelove, A. B.; Anderson, O. P. *J. Am. Chem. Soc.* **1978**, *100*, 3025.
(6) Kuila, D.; Lavallee, D. K.; Schauer, C. K.; Anderson, O. P. *J. Am. Chem. Soc.* **1984**, *106*, 448.
(7) Lavallee, D. K.; White, A.; Diaz, A.; Battioni, J.-P.; Mansuy, D., submitted for publication.
(8) (a) Badet, B. These D'Etat, Université Pierre et Marie Curie, Paris, 1980. (b) Badet, B.; Julia, M. *Tetrahedron Lett.* **1979**, *13*, 1101.
(9) Adler, A. D.; Longo, F. R.; Finarelli, J. E.; Goldmacher, J.; Assour, J.; Korsakoff, L. *J. Org. Chem.* **1967**, *32*, 476.
(10) Bain, M. J.; Lavallee, D. K. *J. Chem. Educ.* **1976**, *53*, 221.

0002-7863/87/1509-3922$01.50/0

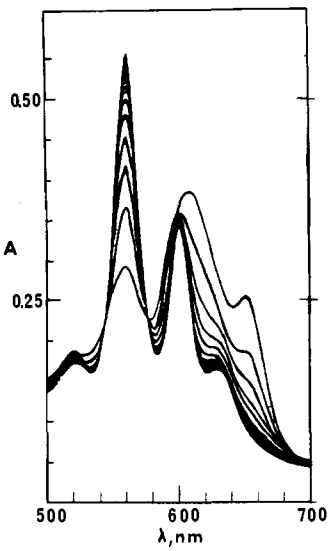

Figure 1. Visible spectra for the reaction of the chlorozinc complex of *N*-Bz-TPP with 1.0 M di-*n*-butylamine in acetonitrile at 25 °C. Spectra were taken at intervals of 4 h.

[Zn(*N*-Ph-TPP)Cl] was synthesized from *N*-phenyltetraphenylporphyrin (made from ClFeTPP by the method of Ortiz de Montellano,[11] with the exception that phenyllithium was used in place of phenylmagnesium bromide) and a twofold excess of zinc chloride hydrate in acetonitrile. In both cases, the material used to investigate the nucleophilic displacement reaction with di-*n*-butylamine exhibited the same visible spectrum as the samples for which elemental analyses and structure determinations were carried out.

Kinetics Experiments. Acetonitrile and di-*n*-butylamine (Fisher ACS Certified Grade) were dried and distilled by literature procedures.[12] Data were obtained by using a Beckman DU8 spectrophotometer equipped with a Peltier solid-state thermostat and with a Varian 635D spectrophotometer thermostated with a Fisher Model 90 circulating bath. Stock solutions were allowed to equilibrate in the spectrophotometer for at least 30 min before kinetic runs were initiated. Cuvettes containing solvent were monitored by using an internal thermocouple to ensure that sufficient time had elapsed for thermal equilibration.

In all reactions, di-*n*-butylamine was present in an excess sufficient to achieve pseudo-first-order conditions. During the displacement of the *N*-benzyl moiety of [Zn(*N*-Bz-TPP)Cl], multiple scans in the region from 500 to 700 nm (see Figure 1) showed the presence of two well-behaved isosbestic points, at 544 and 578 nm. These isosbestic points, like those found previously in the reaction of [Zn(*N*-Me-TPP)Cl], are found throughout the entire course of the reaction and for the entire concentration range of di-*n*-butylamine that was used. Observed pseudo-first-order rate constants were independent of wavelength or direction of absorptivity change and were independent of the initial concentration of the complex (from 4×10^{-5} to 2×10^{-4} M). The spectrum of the product is that of (tetraphenylporphinato)zinc(II) and is the same spectrum as that obtained in the dealkylation reaction for [Zn(*N*-Me-TPP)Cl].[13] Data were analyzed using programs available in the PROPHET computing system.[14]

The rate of the displacement reaction for [Zn(*N*-Ph-TPP)Cl] was studied by withdrawing aliquots (50 μL, using an automatic pipette) from refluxing acetonitrile solutions of the complex and 1.0 or 2.0 M di-*n*-butylamine. These aliquots were diluted to 1.0 mL, and spectra (corrected for solvent absorption) were taken from 500 to 700 nm at 25 °C by using the Beckman DU8 spectrophotometer. Reproducibility was checked by withdrawing multiple aliquots at the same time. The refluxing solutions were kept in a darkened fume hood in vessels surrounded by aluminum foil to prevent exposure of the reactants to light.

Structure Determination for [Zn(*N*-Bz-TPP)Cl]. Crystal data, together with details of the X-ray diffraction experiment and subsequent computations, are listed in Table I. The cell dimensions were obtained from a least-squares fit to the setting angles for 25 reflections (2θ(av) = 21.12°) on a Nicolet R3m diffractometer.[15] The stability of the crystal was monitored during data collection by measurement of the intensities of three standard reflections (511, 030, 247) every 100 data points. Wyckoff ω scans were used to provide rapid intensity measurements, as the crystals eventually cracked at the low temperature employed for the data collection. The intensities of these three reflections did not change significantly during data collection. Lorentz and polarization corrections were performed. A numerical absorption correction was carried out for this platelike crystal; minimum and maximum transmission factors were 0.75 and 0.94, respectively.

The structure was solved using the direct methods routine SOLV.[15] Neutral atom scattering factors[16] and anomalous scattering contributions[17] were used for all atoms. After all atoms of the [Zn(*N*-Bz-TPP)Cl] molecule had been positioned, a difference electron density map revealed the presence of additional electron density. The peaks present were interpreted as representing a pair of independent, disordered CH_3CN solvent molecules. A molecule of methylene chloride also resided at each of the CH_3CN sites a small fraction of the time. Refinement of site occupancy factors (x and $1 - x$) for these fractional atoms yielded a value of approximately 0.8 for the acetonitrile molecules (and thus 0.2 for the methylene chloride molecules). The values of these site occupancy factors were fixed at these levels during the final refinement

Table I. The Crystallographic Experiments and Computations

compd	Zn(*N*-Bz-TPP)Cl	Zn(*N*-Ph-TPP)Cl
formula	$C_{51}H_{35}N_4ClZn$	$C_{50}H_{33}N_4ClZn$
fw, amu	804.7	790.6
temp, °C	−130	20
cryst system	triclinic	orthorhombic
space group	$P\bar{1}$	$P2_12_12_1$
a, Å	10.579 (2)	15.078 (5)
b, Å	12.310 (2)	15.272 (5)
c, Å	17.957 (3)	17.268 (5)
α, deg	85.31 (1)	90
β, deg	80.89 (1)	90
γ, deg	72.63 (1)	90
V, Å^3	2202	3976
Z	2	4
F(000)	832 (no solv)	1632
D_{calcd}, g cm^{-3}	1.21 (no solv)	1.32
cryst dimens, mm	0.31 (100 → $\bar{1}$00) × 0.44 (010 → 0$\bar{1}$0) × 0.08 (001 → 00$\bar{1}$)	0.37 (10$\bar{1}$ → $\bar{1}$01) × 0.44 (010 → 0$\bar{1}$0) × 0.15 (101 → $\bar{1}$0$\bar{1}$)
radiatn	Mo Kα (λ = 0.7107 Å)	Mo Kα
monochromator	graphite	graphite
μ, cm^{-1}	7.2	7.4
scan type	ω (Wyckoff)	$\theta/2\theta$
geometry	bisecting	bisecting
2θ range, deg	3.5–50.0	3.5–50.0
indices collected	$0 \le h \le 13$, $-15 \le k \le 15$, $-22 \le l \le 22$	$-18 \le h \le 0$, $0 \le k \le 19$, $-21 \le l \le 0$
reflectns	8217 measd, 5576 used ($I > 2\sigma(I)$)	4319 measd, 2984 used ($I > 2\sigma(I)$)
scan speed, deg min^{-1}	variable (5–29)	variable (1–29)
no. of least-squares params	604	457
data/parameters	9.23	6.53
R^a	0.052	0.058
$R_w{}^a$	0.061	0.079
GOF^a	1.21	0.89
g	1×10^{-3}	6.9×10^{-3} (refined)
slope, norm prob plot^b	1.06	0.74

$^a R = (\sum||F_o| - |F_c||)/(\sum|F_o|)$; $R_w = \{(\sum w|F_o - F_c|^2)/(\sum w(F_o)^2)\}^{1/2}$; GOF = $\{(\sum w(|F_o| - |F_c|)^2)/(N_{data} - N_{params})\}^{1/2}$. ^{b}Abrahams, S. C. *Acta Crystallogr., Sect. B: Struct. Crystallogr. Cryst. Chem.* **1974**, *B30*, 261–268.

(11) Ortiz de Montellano, P. R.; Kunze, K. L. *J. Am. Chem. Soc.* **1981**, *103*, 6534.
(12) Perrin, D. D.; Armarego, W. L. F.; Perrin, D. R. *Purification of Laboratory Chemicals*; Pergamon: London, 1966.
(13) Lavallee, D. K. *Inorg. Chem.* **1977**, *16*, 955.
(14) The PROPHET computing system is a multisite network, the CBIS system of NIH, which includes a wide variety of statistics and simulation software. We are grateful to the NIH for the installation of the Hunter College facility.
(15) Software used for diffractometer operations was provided with the Nicolet R3m diffractometer. All crystallographic computations were carried out by using the SHELXTL program library (written by G. M. Sheldrick and supplied by Nicolet XRD for the Data General Eclipse S/140 computer in the crystallography laboratory at Colorado State University).
(16) *International Tables for X-Ray Crystallography*; Kynoch: Birmingham, England, 1974; Vol. IV, p 99.
(17) Reference 16, p 149.

cycles. Efflorescence of these solvent molecules was responsible for the rapid shattering of the crystals when removed from the mother liquor at room temperature. Low-temperature data collection was necessary to prevent this crystal degradation.

In the final structural model, all non-hydrogen atoms were given anisotropic thermal parameters. Hydrogen atoms were included in idealized positions (C–H = 0.96 Å, U(H) = 1.2 U_{iso}(C)) on carbon atoms of the [Zn(*N*-Bz-TPP)Cl] molecule. The weighted ($w = [\sigma^2(F_o) + |g|F_o^2]^{-1}$) refinement on F converged ($(\text{shift/esd})_{av} < 0.011$ over the last 12 cycles, $(\text{shift/esd})_{max} = 0.057$ for x of C73 of an occluded solvent molecule) to yield the residual indices shown in Table I. In the final difference electron density map, the highest peak (0.8 e Å^{-3}) occurred between Cl2 and Cl3 and is probably the carbon atom of that partial methylene chloride solvent molecule; the minimum in the map was −0.5 e Å^{-3}.

Fractional atomic coordinates for all non-hydrogen atoms of [Zn(*N*-Bz-TPP)Cl] may be found in Table II. Bond lengths and angles are listed in Table III. Anisotropic thermal parameters (Table S-I), calculated hydrogen atom coordinates (Table S-II), least-squares planes (Table S-III), and structure factors (calculated and observed, ×10, Table S-IV) have been included as supplementary material.

Structure Determination for [Zn(*N*-Ph-TPP)Cl]. Crystal data, together with details of the X-ray diffraction experiment and subsequent computations, are listed in Table I. The cell dimensions were obtained from a least-squares fit to the setting angles for 17 reflections (2θ(av) = 21.76°) on a Nicolet R3m diffractometer.[15] The stability of the crystal was monitored during data collection by measurement of the intensities of three standard reflections (600, 0 10 0, 008) every 197 data points. The intensities of these three reflections declined by approximately 10% during data collection; a correction for this decay was applied (in addition to Lorentz and polarization corrections) during data reduction. No correction was made for absorption, due to the small average value of μt.

The structure was solved by using the direct methods routine SOLV.[15] Neutral atom scattering factors[16] and anomalous scattering contributions[17] were used for all atoms. In the final structural model, all non-hydrogen atoms were given anisotropic thermal parameters. The phenyl rings attached to the meso carbon atoms of the porphyrin core were treated as rigid, hexagonal groups, with all C–C distances constrained to equal 1.395 Å. Hydrogen atoms were included in idealized positions (C–H = 0.96 Å, U(H) = 1.2U_{iso}(C)). The weighted ($w = [\sigma^2(F_o) + |g|F_o^2]^{-1}$) refinement on F converged ($(\text{shift/esd})_{av} < 0.053$ over the last nine cycles) to yield the residual indices given in Table I. In the final difference electron density map, the highest peak (0.79 e Å^{-3}) occurred near (1.0 Å) the zinc(II) atom; the minimum in the map was −0.58 e Å^{-3}.

Final fractional atomic coordinates for all non-hydrogen atoms of [Zn(*N*-Ph-TPP)Cl] may be found in Table IV. Bond lengths and angles are listed in Table V. Anisotropic thermal parameters (Table S-V), calculated hydrogen atom coordinates (Table S-VI), least-squares planes (Table S-VII), and structure factors (calculated and observed, ×10, Table S-VIII) have been included as supplementary material.

Results and Discussion

Relative Reactivity of N-Substituted Zn(II) Porphyrin Complexes. The rate law for the nucleophilic displacement reaction of [Zn(*N*-Bz-TPP)Cl] with di-*n*-butylamine in acetonitrile (Table VI) is first order in the amine, as previously observed for the *N*-methyl complex.[18] Under pseudo-first-order conditions, with nucleophile (di-*n*-butylamine) in excess, the reaction is also first-order in the zinc complex.

The corresponding *N*-phenyl complex is extremely unreactive. Solutions of the *N*-phenvl complex and di-*n*-butylamine (up to 2.0 M) were subjected to reflux conditions in acetonitrile (protected from light) for 3 weeks. Aliquots withdrawn throughout this period showed no detectable change in the visible absorption spectrum. A change of 10% would be readily detected under these conditions. When the expected product of the nucleophilic displacement reaction (Zn(TPP)) is refluxed under the same conditions, it does not decompose. Therefore, if Zn(TPP) were formed, it would be evident in the visible absorption spectrum of the reaction mixture.

Kinetic results for the dealkylation of *N*-methylporphyrins with several different metal ions have been reported,[18,19] but the only ion for which a variety of *N*-substituents has been investigated is copper(II).[4] The fact that the rate of nucleophilic displacement of the *N*-substituent is highly dependent on the stability of the metalloporphyrin product and, in the case of the copper(II) complexes we have studied, on the ability of the N-substituent

Table II. Atomic Coordinates (Fractional, ×10^4)[a] and Isotropic Thermal Parameters (Å^2 × 10^3)[b] for [Zn(*N*-Bz-TPP)Cl]

atom	x	y	z	U_{iso}
Zn	8812.9 (5)	6966.5 (4)	1962.9 (3)	15.4 (2)
Cl1	9319 (1)	7916.8 (9)	2848.0 (6)	24.2 (4)
N1	6942 (3)	6523 (3)	2822 (2)	16 (1)
N2	9704 (3)	5250 (3)	2201 (2)	16 (1)
N3	9804 (3)	6777 (3)	900 (2)	17 (1)
N4	7209 (3)	8176 (2)	1543 (2)	15 (1)
C1	6003 (4)	7543 (3)	3093 (2)	17 (1)
C2	5846 (4)	7465 (4)	3893 (2)	22 (2)
C3	6689 (4)	6453 (3)	4111 (2)	22 (2)
C4	7392 (4)	5869 (3)	3469 (2)	16 (1)
C5	8480 (4)	4875 (3)	3448 (2)	17 (1)
C6	9490 (4)	4574 (3)	2835 (2)	17 (1)
C7	10530 (4)	3508 (3)	2801 (2)	19 (1)
C8	11385 (4)	3547 (3)	2175 (2)	17 (1)
C9	10898 (4)	4630 (3)	1796 (2)	15 (1)
C10	11521 (4)	4969 (3)	1111 (2)	18 (1)
C11	10991 (4)	5962 (3)	687 (2)	18 (1)
C12	11573 (4)	6266 (3)	−56 (2)	22 (2)
C13	10713 (4)	7233 (3)	−287 (2)	21 (2)
C14	9602 (4)	7552 (3)	312 (2)	17 (1)
C15	8462 (4)	8484 (3)	290 (2)	16 (1)
C16	7342 (4)	8749 (3)	851 (2)	16 (1)
C17	6138 (4)	9650 (3)	782 (2)	20 (1)
C18	5295 (4)	9639 (3)	1424 (2)	20 (1)
C19	5974 (4)	8728 (3)	1904 (2)	18 (1)
C20	5441 (4)	8482 (3)	2645 (2)	16 (1)
C21	6555 (4)	5906 (3)	2244 (2)	18 (1)
C22	5227 (4)	5671 (3)	2506 (2)	20 (1)
C23	5138 (5)	4746 (4)	2973 (3)	36 (2)
C24	3876 (6)	4595 (5)	3250 (3)	50 (3)
C25	2735 (5)	5392 (5)	3031 (3)	47 (2)
C26	2828 (5)	6273 (4)	2557 (3)	42 (2)
C27	4049 (4)	6424 (4)	2299 (3)	30 (2)
C30	8620 (4)	4171 (3)	4159 (2)	18 (1)
C31	9777 (4)	3939 (3)	4497 (2)	20 (1)
C32	9890 (4)	3293 (3)	5168 (2)	24 (2)
C33	8862 (4)	2872 (4)	5507 (2)	27 (2)
C34	7709 (5)	3097 (4)	5183 (3)	34 (2)
C35	7583 (4)	3744 (4)	4511 (2)	30 (2)
C40	12854 (4)	4204 (3)	800 (2)	17 (1)
C41	13038 (4)	3629 (3)	138 (2)	21 (1)
C42	14292 (4)	2937 (3)	−146 (2)	24 (2)
C43	15371 (4)	2810 (4)	226 (3)	32 (2)
C44	15199 (4)	3363 (4)	894 (3)	34 (2)
C45	13948 (4)	4056 (4)	1174 (2)	25 (2)
C50	8411 (4)	9248 (3)	−409 (2)	16 (1)
C51	8361 (4)	8823 (4)	−1095 (2)	23 (2)
C52	8356 (4)	9492 (4)	−1749 (2)	25 (2)
C53	8388 (4)	10597 (4)	−1731 (2)	23 (2)
C54	8441 (4)	11032 (4)	−1056 (2)	23 (2)
C55	8450 (4)	10355 (3)	−397 (2)	19 (1)
C60	4228 (4)	9338 (3)	3031 (2)	17 (1)
C61	3139 (4)	9003 (3)	3383 (2)	20 (1)
C62	2045 (4)	9776 (4)	3773 (2)	28 (2)
C63	2045 (4)	10885 (4)	3825 (2)	30 (2)
C64	3125 (5)	11237 (4)	3481 (2)	30 (2)
C65	4214 (4)	10475 (3)	3078 (2)	25 (2)
C71(0.8)[c]	8077 (7)	695 (5)	1906 (4)	42 (3)
C72(0.8)	7993 (6)	1713 (7)	2241 (4)	46 (3)
N5(0.8)	7960 (7)	2550 (7)	2484 (5)	96 (4)
Cl2(0.2)	8579 (11)	1509 (10)	3135 (6)	101 (5)
Cl3(0.2)	7190 (12)	1389 (14)	1921 (6)	112 (7)
C73(0.8)	7319 (14)	−108 (15)	4220 (8)	185 (9)
C74(0.8)	6307 (12)	1230 (9)	4241 (5)	100 (5)
N6(0.8)	5469 (7)	1944 (7)	4302 (4)	81 (4)
Cl4(0.2)	6103 (26)	545 (20)	4499 (10)	260 (16)
Cl5(0.2)	8246 (17)	501 (16)	4121 (8)	166 (9)

[a] Estimated standard deviations in the least significant digits are given in parentheses. [b] The equivalent isotropic U_{iso} value is defined as one-third of the trace of the U tensor. [c] This atom and those following were found at site occupancy levels given in parentheses.

(18) Lavallee, D. K. *Inorg. Chem.* **1976**, *15*, 691.
(19) (a) Doi, J. D.; Compito-Magliozzo, C.; Lavallee, D. K. *Inorg. Chem.* **1984**, *23*, 79. (b) Kuila, D.; Lavallee, D. K. *Inorg. Chem.* **1983**, *22*, 1095.

Table III. Selected Bond Lengths (Å) and Angles (deg) for [Zn(*N*-Bz-TPP)Cl][a]

a. Bond Lengths

Zn–Cl1	2.265 (1)	N3–C11	1.373 (4)
Zn–N1	2.477 (3)	C11–C12	1.447 (5)
Zn–N2	2.080 (3)	C12–C13	1.344 (5)
Zn–N3	2.023 (3)	C13–C14	1.444 (5)
Zn–N4	2.092 (3)	C14–N3	1.363 (5)
N1–C1	1.416 (4)	C11–C10	1.401 (5)
C1–C2	1.419 (5)	C14–C15	1.397 (5)
C2–C3	1.367 (5)	N4–C16	1.386 (5)
C3–C4	1.395 (5)	C16–C17	1.432 (5)
C4–N1	1.420 (5)	C17–C18	1.345 (5)
C1–C20	1.388 (5)	C18–C19	1.439 (5)
C4–C5	1.406 (5)	C19–N4	1.365 (4)
N2–C6	1.384 (5)	C16–C15	1.404 (5)
C6–C7	1.437 (5)	C19–C20	1.406 (5)
C7–C8	1.335 (5)	N1–C21	1.506 (6)
C8–C9	1.435 (5)	C21–C22	1.513 (6)
C9–N2	1.390 (4)	C22–C23	1.376 (6)
C6–C5	1.396 (5)	C23–C24	1.409 (9)
C9–C10	1.395 (5)	C24–C25	1.398 (8)
		C25–C26	1.339 (8)
		C26–C27	1.363 (7)
		C27–C22	1.396 (5)

b. Bond Angles

Cl1–Zn–N1	93.2 (1)	C11–N3–Zn	125.2 (2)
Cl1–Zn–N2	105.5 (1)	C14–N3–Zn	126.6 (2)
Cl1–Zn–N3	123.5 (1)	C11–N3–C14	106.8 (3)
Cl1–Zn–N4	103.3 (1)	N3–C11–C12	109.4 (3)
N1–Zn–N2	80.4 (1)	N3–C11–C10	125.1 (3)
N1–Zn–N3	143.3 (1)	C10–C11–C12	125.5 (3)
N1–Zn–N4	80.9 (1)	C11–C12–C13	106.9 (3)
N2–Zn–N3	89.4 (1)	C12–C13–C14	107.4 (3)
N2–Zn–N4	146.4 (1)	C13–C14–N3	109.6 (3)
N3–Zn–N4	89.1 (1)	C13–C14–C15	126.0 (3)
C1–N1–Zn	109.9 (2)	N3–C14–C15	124.4 (3)
C4–N1–Zn	111.5 (2)	C14–C15–C16	125.9 (3)
C1–N1–C4	106.2 (3)	C16–N4–Zn	122.9 (2)
C1–N1–C21	117.5 (3)	C19–N4–Zn	130.0 (2)
C4–N1–C21	116.5 (3)	C16–N4–C19	105.8 (3)
Zn–N1–C21	94.9 (2)	N4–C16–C17	109.6 (3)
N1–C1–C2	107.8 (3)	N4–C16–C15	126.0 (3)
N1–C1–C20	125.1 (3)	C15–C16–C17	124.4 (3)
C2–C1–C20	126.9 (3)	C16–C17–C18	107.4 (3)
C1–C2–C3	108.5 (3)	C17–C18–C19	107.1 (3)
C2–C3–C4	108.9 (3)	C18–C19–N4	110.1 (3)
C3–C4–N1	108.6 (3)	C18–C19–C20	124.1 (3)
C3–C4–C5	126.3 (4)	N4–C19–C20	125.8 (3)
N1–C4–C5	124.6 (3)	C19–C20–C1	125.5 (3)
C4–C5–C6	124.4 (3)	N1–C21–C22	112.1 (3)
C6–N2–Zn	130.5 (2)	C21–C22–C23	121.4 (4)
C9–N2–Zn	122.5 (2)	C22–C23–C24	120.0 (4)
C6–N2–C9	105.4 (3)	C23–C24–C25	118.6 (5)
N2–C6–C5	126.7 (3)	C24–C25–C26	121.2 (5)
N2–C6–C7	109.7 (3)	C25–C26–C27	120.0 (5)
C5–C6–C7	123.4 (3)	C26–C27–C22	121.8 (4)
C6–C7–C8	107.6 (3)	C27–C22–C21	120.2 (4)
C7–C8–C9	107.7 (3)	C27–C22–C23	118.4 (4)
C8–C9–N2	109.5 (3)		
C8–C9–C10	124.1 (3)		
N2–C9–C10	126.3 (3)		

[a] Estimated standard deviations in the least significant digits are given in parentheses.

Table IV. Atomic Coordinates (Fractional, $\times 10^4$)[a] and Isotropic Thermal Parameters ($Å^2 \times 10^3$)[b] for [Zn(*N*-Ph-TPP)Cl]

atom	*x*	*y*	*z*	U_{iso}
Zn	4805.4 (5)	6017.5 (4)	1365.3 (4)	38.5 (2)
Cl	5034 (1)	5579 (1)	2579 (1)	61.9 (6)
N1	4788 (4)	7621 (3)	1634 (3)	40 (2)
N2	3444 (3)	6277 (3)	1214 (3)	38 (2)
N3	4720 (4)	5109 (3)	518 (4)	48 (2)
N4	6047 (3)	6374 (3)	934 (3)	38 (2)
C1	5581 (4)	7831 (4)	2015 (4)	42 (2)
C2	5365 (4)	8136 (4)	2748 (4)	45 (2)
C3	4469 (5)	8103 (4)	2856 (4)	49 (2)
C4	4079 (4)	7775 (4)	2181 (4)	40 (2)
C5	3193 (4)	7569 (4)	2036 (4)	42 (2)
C6	2914 (4)	6932 (4)	1511 (4)	45 (2)
C7	2016 (5)	6798 (5)	1269 (5)	53 (2)
C8	1985 (4)	6049 (5)	858 (5)	53 (2)
C9	2872 (4)	5718 (4)	836 (4)	43 (2)
C10	3113 (4)	4907 (5)	481 (4)	46 (2)
C11	3969 (5)	4648 (4)	333 (4)	47 (2)
C12	4224 (5)	3895 (5)	−135 (5)	67 (3)
C13	5103 (5)	3928 (5)	−232 (5)	63 (3)
C14	5408 (5)	4723 (4)	162 (5)	52 (2)
C15	6257 (5)	5052 (5)	109 (4)	49 (2)
C16	6526 (4)	5878 (4)	413 (4)	44 (2)
C17	7343 (5)	6320 (5)	214 (5)	58 (3)
C18	7362 (5)	7064 (5)	622 (5)	58 (3)
C19	6591 (4)	7093 (4)	1094 (4)	44 (2)
C20	6424 (4)	7723 (4)	1671 (4)	41 (2)
C21	4675 (4)	8057 (4)	869 (4)	37 (2)
C22	4665 (4)	7614 (5)	195 (4)	47 (2)
C23	4634 (5)	8070 (5)	−520 (4)	57 (3)
C24	4632 (5)	8968 (5)	−522 (5)	65 (3)
C25	4657 (5)	9423 (5)	192 (5)	68 (3)
C26	4675 (5)	8980 (4)	871 (4)	51 (2)
C30	2509 (4)	8013 (3)	2534 (3)	51 (2)
C31	2522 (4)	8921 (3)	2619 (3)	68 (3)
C32	1852 (4)	9341 (3)	3033 (3)	96 (5)
C33	1167 (4)	8853 (3)	3363 (3)	88 (4)
C34	1153 (4)	7945 (3)	3279 (3)	77 (4)
C35	1824 (4)	7525 (3)	2864 (3)	65 (3)
C40	2376 (5)	4328 (4)	222 (3)	48 (2)
C41	2054 (5)	4385 (4)	−533 (3)	118 (6)
C42	1364 (5)	3840 (4)	−772 (3)	121 (6)
C43	996 (5)	3238 (4)	−256 (3)	101 (5)
C44	1319 (5)	3181 (4)	499 (3)	149 (7)
C45	2009 (5)	3726 (4)	739 (3)	106 (5)
C50	6926 (5)	4529 (5)	−332 (3)	59 (3)
C51	7456 (5)	3939 (5)	75 (3)	109 (5)
C52	8096 (5)	3449 (5)	−316 (3)	153 (8)
C53	8206 (5)	3549 (5)	−1113 (3)	105 (5)
C54	7676 (5)	4140 (5)	−1520 (3)	144 (7)
C55	7035 (5)	4629 (5)	−1129 (3)	117 (6)
C60	7162 (3)	8266 (3)	1978 (3)	52 (3)
C61	8010 (3)	7922 (3)	2083 (3)	64 (3)
C62	8704 (3)	8466 (3)	2316 (3)	92 (4)
C63	8548 (3)	9355 (3)	2444 (3)	95 (5)
C64	7700 (3)	9699 (3)	2339 (3)	85 (4)
C65	7007 (3)	9155 (3)	2106 (3)	57 (3)

[a] Estimated standard deviations in the least significant digits are given in parentheses. [b] The equivalent isotropic U_{iso} value is defined as one-third of the trace of the U tensor.

to form a stable carbocation, has led us to conclude that the transition state of the displacement reaction closely resembles the structure of the products.[19b] A comparison of the activation parameters for the reactions of copper(II) and zinc(II) complexes (Table VII) indicates that this conclusion is also valid for the reactions of the zinc(II) complexes. There is a striking compensation effect (the compensation of a less favorable $\Delta H^{\ddagger}$ by a more favorable $\Delta S^{\ddagger}$) in the comparison between Zn(*N*-Bz-TPP)Cl and Zn(*N*-Me-TPP)Cl. For these two complexes, the differences in values of $\Delta H^{\ddagger}$ ($\Delta(\Delta H^{\ddagger})$ = 106 kJ mol^{-1}) and $\Delta S^{\ddagger}$ ($\Delta(\Delta S^{\ddagger})$ = 322 J mol^{-1} K^{-1}) are large, but the difference in $\Delta G^{\ddagger}$ ($\Delta(\Delta G^{\ddagger})$ = 5 kJ mol^{-1}) is small. Thus, the $\Delta G^{\ddagger}$ values for the zinc(II) and copper(II) complexes are remarkably similar, despite the great differences in their reactivities near ambient temperature.

The reaction by which the N-substituent of N-substituted porphyrins is displaced is unusual in that the bond between a carbon atom and a pyrrolic nitrogen atom can be cleaved under relatively mild conditions. The driving force for these reactions is provided by the formation of the more stable non-N-substituted porphyrin product. *N*-Methylporphyrin complexes contain three metal–nitrogen bonds of approximately the same length as the bonds in non-N-substituted metalloporphyrins of the same metal ion, and one metal–nitrogen bond that is much longer.[20] On the

(20) Anderson, O. P.; Kopelove, A. B; Lavallee, D. K. *Inorg. Chem.* **1980**, *19*, 2101.

Table V. Selected Bond Lengths (Å) and Angles (deg) for [Zn(*N*-Ph-TPP)Cl][a]

a. Bond Lengths

Zn-Cl	2.227 (2)	N3-C11	1.371 (9)
Zn-N1	2.492 (6)	C11-C12	1.46 (1)
Zn-N2	2.107 (5)	C12-C13	1.34 (1)
Zn-N3	2.020 (6)	C13-C14	1.46 (1)
Zn-N4	2.087 (5)	C14-N3	1.342 (9)
N1-C1	1.402 (9)	C11-C10	1.37 (1)
C1-C2	1.388 (9)	C14-C15	1.38 (1)
C2-C3	1.36 (1)	N4-C16	1.381 (8)
C3-C4	1.40 (1)	C16-C17	1.45 (1)
C4-N1	1.446 (9)	C17-C18	1.34 (1)
C1-C20	1.411 (9)	C18-C19	1.42 (1)
C4-C5	1.395 (9)	C19-N4	1.398 (8)
N2-C6	1.379 (8)	C16-C15	1.43 (1)
C6-C7	1.43 (1)	C19-C20	1.408 (9)
C7-C8	1.35 (1)	N1-C21	1.490 (8)
C8-C9	1.431 (9)	C21-C22	1.346 (9)
C9-N2	1.377 (8)	C22-C23	1.42 (1)
C6-C5	1.395 (9)	C23-C24	1.37 (1)
C9-C10	1.429 (9)	C24-C25	1.42 (1)
		C25-C26	1.35 (1)
		C26-C21	1.409 (9)

b. Bond Angles

Cl-Zn-N1	97.0 (2)	C11-N3-Zn	125.1 (5)
Cl-Zn-N2	108.9 (2)	C14-N3-Zn	125.7 (5)
Cl-Zn-N3	119.0 (2)	C11-N3-C14	107.8 (6)
Cl-Zn-N4	106.0 (2)	N3-C11-C12	108.5 (6)
N1-Zn-N2	80.1 (2)	N3-C11-C10	125.7 (6)
N1-Zn-N3	144.0 (2)	C10-C11-C12	125.4 (7)
N1-Zn-N4	79.6 (2)	C11-C12-C13	107.6 (7)
N2-Zn-N3	88.7 (2)	C12-C13-C14	106.5 (7)
N2-Zn-N4	141.4 (2)	C13-C14-N3	109.5 (6)
N3-Zn-N4	88.8 (2)	C13-C14-C15	124.2 (7)
C1-N1-Zn	107.7 (5)	N3-C14-C15	126.0 (6)
C4-N1-Zn	106.8 (5)	C14-C15-C16	124.2 (6)
C1-N1-C4	106.7 (5)	C16-N4-Zn	124.0 (4)
C1-N1-C21	114.3 (5)	C19-N4-Zn	131.3 (4)
C4-N1-C21	115.0 (5)	C16-N4-C19	104.6 (5)
Zn-N1-C21	106.0 (5)	N4-C16-C17	110.2 (6)
N1-C1-C2	107.7 (6)	N4-C16-C15	125.2 (6)
N1-C1-C20	123.0 (6)	C15-C16-C17	124.6 (6)
C2-C1-C20	129.4 (6)	C16-C17-C18	106.8 (7)
C1-C2-C3	110.2 (6)	C17-C18-C19	108.1 (7)
C2-C3-C4	108.4 (6)	C18-C19-N4	110.0 (6)
C3-C4-N1	106.9 (6)	C18-C19-C20	125.0 (6)
C3-C4-C5	129.4 (6)	N4-C19-C20	124.9 (6)
N1-C4-C5	123.6 (6)	C19-C20-C1	122.6 (6)
C4-C5-C6	124.3 (6)	N1-C21-C22	122.9 (5)
C6-N2-Zn	130.9 (4)	C21-C22-C23	120.4 (7)
C9-N2-Zn	123.5 (4)	C22-C23-C24	119.5 (7)
C6-N2-C9	105.3 (5)	C23-C24-C25	119.3 (8)
N2-C6-C5	125.0 (6)	C24-C25-C26	120.6 (7)
N2-C6-C7	109.6 (6)	C25-C26-C21	119.8 (7)
C5-C6-C7	125.1 (6)	C26-C21-C22	120.4 (6)
C6-C7-C8	107.9 (6)	C26-C21-N1	116.4 (6)
C7-C8-C9	106.4 (6)		
C8-C9-N2	110.7 (6)		
C8-C9-C10	123.7 (6)		
N2-C9-C10	125.5 (6)		

[a] Estimated standard deviations in the least significant digits are given in parentheses.

basis of the evidence presently available, axial ligation of metals in N-substituted porphyrin complexes is limited to one (with the exception of a complex in which an oxygen atom of the N-substituent forms a bond to a coordinated iron(II) atom[21]), while among non-N-substituted porphyrins there are commonly two axial ligands, providing a total of six strong bonds. Thus, displacement of the N-substituent will lead to at least one stronger metal–nitrogen bond and, often, to a bond to a second axial ligand. Under the conditions we have commonly employed for nucleophilic

(21) Mansuy, D.; Battioni, J.-P.; Akhrem, I.; Dupre, D.; Fischer, J.; Weiss, R.; Morgenstern-Badarau, I. *J. Am. Chem. Soc.* **1984**, *106*, 6112.

Table VI. Rate Constants for the Reactions of [Zn(*N*-Bz-TPP)Cl] with Di-*n*-butylamine in Acetonitrile[a]

T, °C	10^5[complex], M	[amine], M	$10^5 k_{obsd}$, s^{-1}	$10^5 k$, $M^{-1}\ s^{-1}$
25	5.4	0.40	2.28	5.70
25	5.7	0.40	2.25	5.63
25	7.4	0.40	2.63	6.58
25	7.7	0.40	2.65	6.62
45	3.6	1.33	29.0	21.8
45	5.4	1.00	26.0	26.0
45	5.9	0.80	20.3	26.0
45	6.4	0.67	13.8	21.5
45	6.5	0.67	14.4	20.6
45	8.7	0.40	11.2	28.0
45	17	0.40	11.7	29.2
45	9.5	0.22	7.2	32.7
45	9.8	0.22	7.1	32.3
65	3.9	0.40	90	225
65	4.3	0.40	73	183
65	7.7	0.40	85	212
65	7.9	0.40	79	198

[a] All runs fit a rate law that is first order in porphyrin concentration, with a correlation coefficient of at least 0.998. The maximum difference between observed and calculated absorbance readings was 0.003.

Table VII. Rates and Activation Parameters for Nucleophilic Displacement of the N-Substituent on N-Substituted Tetraphenylporphyrin Complexes[a]

N-subst	half-life	$\Delta H^{\ddagger}$ kJ mol^{-1}	$\Delta S^{\ddagger}$ J $mol^{-1}\ K^{-1}$	$\Delta G^{\ddagger}$ kJ mol^{-1}
		Zinc Complexes[b]		
benzyl	2 h	71	−92	100
methyl[c]	200 h	176	230	105
phenyl	>200 days			
		Copper Complexes[d,e]		
benzyl	20 ms	63	−46	75
methyl	2 s	71	−54	88
ethyl	20 s	75	−59	92
phenyl	>10 days			

[a] In CH_3CN, with 0.1 *M* di-*n*-butylamine as nucleophile. [b] Half-life at 60 °C. [c] Reference 8b. [d] Half-life at 45 °C. [e] Reference 3.

displacement reactions,[4,13,18] the nucleophile is a dialkylamine, so the pyrrolic nitrogen–carbon bond of the N-substituted reactant is replaced in the products by a bond between the nitrogen atom of an aliphatic amine and a carbon atom.

The marked dependence of the reaction rates on the nature of the N-substituent, the apparent generality of the dependence, and the tendency of the rates to reflect a transition-state structure resembling the products led us to investigate the possibility that the relative reactivities might be reflected in features of the ground-state structures of a series of complexes differing in N-substituents. One would expect that a molecule that exhibits a ground state more like the non-N-substituted metalloporphyrin product of the nucleophilic displacement reaction would display enhanced reactivity. In the case of the chlorozinc(II) complexes of N-substituted porphyrins, such a trend would be characterized by stronger bonding between the metal and the substituted nitrogen atom, weaker bonding of the axial chloride ligand, concomitant changes in the metal–ligand bond angles, and a decreased tilt, or cant, of the N-substituted pyrrole ring with respect to the plane of the remainder of the macrocycle.

Correlation of Reactivity and Structure. The structure of chloro(*N*-methyltetraphenylporphinato)zinc(II), Zn(*N*-Me-TPP)Cl, has been previously reported,[5] and the structure of Zn(*N*-Ph-TPP)Cl has been the subject of a preliminary communication.[6] Figure 2 shows the structures of the Zn(*N*-Bz-TPP)Cl and Zn(*N*-Ph-TPP)Cl complexes, along with the numbering scheme used for those complexes in this report.

Structural parameters for Zn(*N*-Me-TPP)Cl clearly indicated that the zinc(II) atom interacted more weakly with the alkylated nitrogen atom than did other metal atoms.[20] In addition to the long bond between the zinc(II) atom and the methylated nitrogen

Table VIII. Structural Parameters for N-Substituted Zinc Porphyrins

	Zn(*N*-Ph-TPP)Cl	Zn(*N*-Me-TPP)Cl[5]	Zn(*N*-Bz-TPP)Cl
Zn–Cl, Å	2.227 (2)	2.232 (3)	2.265 (1)
Zn–N1, Å	2.492 (6)	2.530 (7)	2.477 (3)
Zn–N2, Å	2.107 (5)	2.089 (6)	2.080 (3)
Zn–N3, Å	2.020 (6)	2.018 (9)	2.023 (3)
Zn–N4, Å	2.087 (5)	2.081 (9)	2.092 (3)
N1–Zn–Cl, deg	97.0 (2)	94.6 (2)	93.2 (1)
Zn–P1,[a] Å	0.67	0.65	0.58
N1 ring cant,[b] deg	42	39	32

[a] P1 is the plane through N2, N3, and N4. [b] With respect to plane P1.

atom, that weaker interaction was manifested in the value of the N 1s binding energy for the substituted nitrogen atom in the X-ray photoelectron spectrum of the zinc complex.[22]

Summarized in Table VIII are some of the structural features of the *N*-phenyl, *N*-methyl, and *N*-benzyl zinc complexes that are relevant to comparison of their relative enthalpies of activation. In the much more reactive *N*-benzyl complex, the zinc atom is found closer to the plane of the three nonsubstituted porphyrin nitrogen atoms (P1 in Table VIII). The chloride ion is more weakly bound in the *N*-benzyl complex than in either of the other two derivatives, and the *N*-benzyl complex exhibits the shortest Zn–N1 distance. The N-substituted pyrrole ring is highly canted in all three zinc complexes, but least so in the reactive *N*-benzyl compound (see Table VIII). In each of the three cases, the sense of the tilt of the N1 pyrrole ring is opposite to that of the other pyrrole rings, which are slightly domed to accommodate bonding between the metal ion and the sp^2-hybridized nitrogen atoms. In non-N-substituted metalloporphyrins, the pyrrole rings either are not canted (square-planar and six-coordinate complexes) or are all canted to essentially the same degree in a slightly domed configuration. The extent of the tilt is a feature that indicates greater tetrahedral character of the metal atom coordination sphere,[20] and, as noted above, it is most pronounced in the *N*-benzyl compound, where the bonding between the metal ion and the N-substituted pyrrole ring is strongest. While most of the structural parameters in these three complexes follow the pattern expected if the ground-state structures parallel reactivity, the Zn–N1 distance in the *N*-methyl complex is unexpectedly long relative to the corresponding distances in the other two compounds.

A ground-state structure that more closely resembles the product of the reaction presumably brings the complex energetically and structurally closer to the transition state. As argued above, such a trend appears evident for the chlorozinc(II) complexes of *N*-benzyl-, *N*-methyl-, and *N*-phenyltetraphenylporphyrin. Thus, although there is no necessary correlation between reactivity and ground-state structure, such a correlation seems to be evident for the N-substituted porphyrin complexes of zinc(II). The observation of similar reactivity patterns for N-substituted porphyrin complexes of copper(II),[4] cobalt(II),[7] nickel(II),[7] and palladium(II),[7] combined with the regular correlation between structural parameters and ionic radii found for a series of *N*-methylporphyrin complexes of Mn(II), Fe(II), Co(II), and Zn(II),[20] provides a basis for expecting that the correlation between ground-state structure and reactivity toward displacement of the N-substituent may be a general one.

Enzyme Inhibition. Dicarboxylate-substituted *N*-alkylporphyrins have been shown to inhibit the enzyme (ferrochelatase) involved in the complexation of iron to form heme, and zinc *N*-alkylprotoporphyrin complexes inhibit heme oxygenase, which is involved in the metabolism of heme to form bile pigments.[3] The inhibition of ferrochelatase is likely to be the reason for the accumulation of iron-free porphyrins in animals treated with drugs that cause the destruction of cytochrome P-450 to form *N*-alkylporphyrins.[1,2] *N*-alkylporphyrins bearing different N-substituents inhibit ferrochelatase to different degrees (larger alkyl groups being less inhibitory). The degree of inhibition also depends on which pyrrole ring is N-substituted, with greater inhibition found when the N-substitution occurs on one of the pyrrole rings bearing propionic acid side chains.

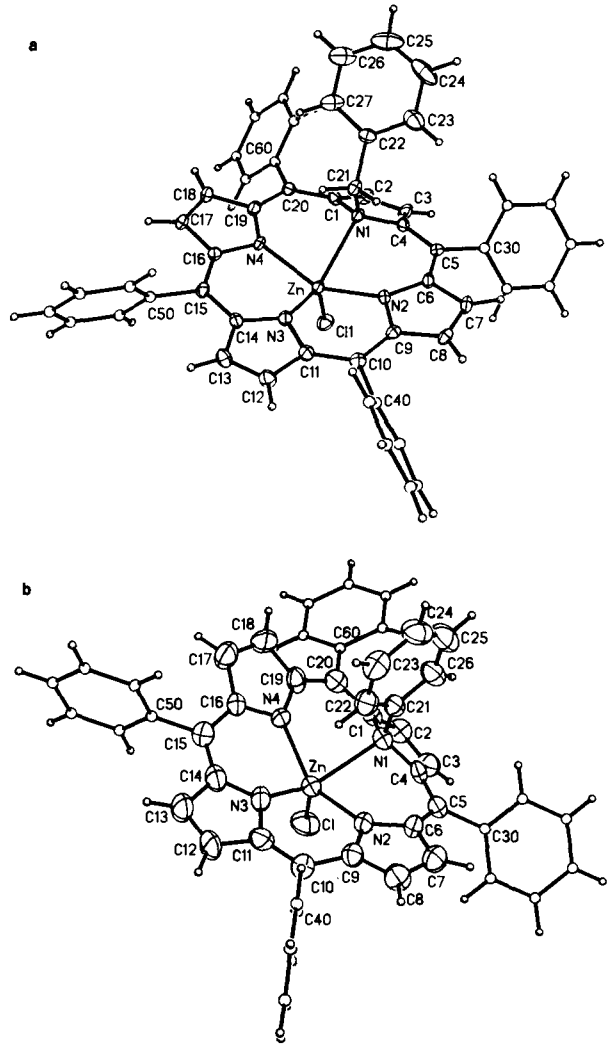

Figure 2. a. A view of the [Zn(*N*-Bz-TPP)Cl] complex, showing the numbering scheme used. Thermal ellipsoids are depicted at the 50% probability level, while carbon atoms of meso phenyl substituents and all hydrogen atoms are drawn as spheres of arbitrary radius for clarity. b. A view of the [Zn(*N*-Ph-TPP)Cl] complex, drawn in a similar fashion.

Such differences between inhibitory properties of the isomers is pronounced for the zinc complexes but not for the free bases of *N*-methyl- and *N*-ethylprotoporphyrins.[23] This effect has been attributed to the greater cant of the N-substituted pyrrole ring for the zinc complex; increased tilt would increase the distance between the propionic acid side chains of the substituted pyrrole and the neighboring pyrrole, making the interaction with the enzyme different. On the basis of the structures of the zinc(II) complexes discussed above and the structure of one of the corresponding free bases,[24] such a structural change seems to provide a plausible explanation for the differences in inhibition exhibited by zinc complexes and the corresponding free bases. The cant of the N-methylated pyrrole ring in the free base of *N*-Me-TPP is only 28°, vs. 39° for the zinc *N*-methyl complex.

It is, of course, possible that unmetallated *N*-alkylporphyrin is bound to the protein in the monoprotonated form. There are two structures that relate to this possibility. The monoprotonated form of *N*-ethylacetoxyoctaethylporphyrin[25] has a pyrrole ring

(22) Lavallee, D. K.; Brace, J.; Winograd, N. *Inorg. Chem.* **1979**, *18*, 1776.

(23) De Matteis, F.; Jackson, A. H.; Gibbs, A. H.; Rao, K. R. N.; Atton, J.; Weerasinghe, S.; Hollands, C. *FEBS Lett.* **1982**, *142*, 44.

(24) Lavallee, D. K.; Anderson, O. P. *J. Am. Chem. Soc.* **1982**, *104*, 4707.

(25) McLaughlin, G. M. *J. Chem. Soc., Perkin Trans. 2* **1974**, 136.

cant of only 19.1°, while this angle for its cobalt complex[26] is 44°, a considerably greater difference than that between the unprotonated free base and its complex.

Metalloporphyrins other than heme are able to bind to heme oxygenase, and zinc complexes act as competitive inhibitors of this enzyme. When De Matteis and co-workers tested the inhibitory ability of a series of zinc *N*-alkylporphyrin complexes, larger N-substituents (ethyl and propyl) were found to be less inhibitory than *N*-methylporphyrins.[3] They proposed that the correlation between structure and inhibition for this enzyme was also related to the cant of the N-substituted pyrrole ring, with larger groups causing a greater tilt. While there are, indeed, substantial differences in the cant of the N-substituted pyrrole ring among the members of the series of N-substituted zinc(II) porphyrins reported herein, these differences are not straightforwardly related to the "bulk" of the N-substituent. In fact, the pyrrole ring for which the N-substituent is a benzyl group is less canted (by 7°) than in the complex with a methyl substituent. In the series of *N*-alkylporphyrins studied by DeMatteis, the N-substituents are very similar (*N*-methyl-, *N*-ethyl-, and *N*-*n*-propyl groups), all involving an *N*-methylene linkage. No substantial difference in the cant of the pyrrole ring is expected for these compounds. On the basis of our results, the differences in heme oxygenase inhibition for the zinc(II) complexes of *N*-alkylprotoporphyrin are due not to the cant of the N-substituted pyrrole ring but instead to the requirement for additional space in the binding pocket to accommodate more bulky N-substituents. The need to accommodate the N-substituent also explains the marked difference in inhibition of ferrochelatase by *N*-*n*-propylprotoporphyrin IX and *N*-*n*-propylmesoporphyrin IX in comparison with the corresponding *N*-methyl and *N*-ethyl free base porphyrins.

(26) Goldberg, D. E.; Thomas, K. M. *J. Am. Chem. Soc.* **1976**, *98*, 913.

Acknowledgment. The Nicolet R3m/E diffractometer and crystallographic computing system at Colorado State University were purchased with funds provided by the National Science Foundation (CHE 81-03011). Work at Hunter College was generously supported by the National Cancer Institute of the NIH (CA 25427) and the PSC-CUNY grants program to D.K.L. and by a NATO grant to D.K.L. and D.M. (583-83). Work at Colorado State University was supported by the National Institute of General Medical Sciences of the NIH (GM 30306) and the Biomedical Research Support Grant program of the NIH.

Supplementary Material Available: Table S-1, anisotropic thermal parameters for [Zn(*N*-Bz-TPP)Cl], Table S-II, calculated hydrogen atom coordinates for [Zn(*N*-Bz-TPP)Cl], Table S-III, least-squares planes for [Zn(*N*-Bz-TPP)Cl], Table S-V, anisotropic thermal parameters for [Zn(*N*-Ph-TPP)Cl], Table S-VI, calculated hydrogen atom coordinates for [Zn(*N*-Ph-TPP)Cl], and Table S-VII, least-squares planes for [Zn(*N*-Ph-TPP)Cl] (14 pages); Table S-IV, observed and calculated structure factors for [Zn(*N*-Bz-TPP)Cl], and Table S-VIII, observed and calculated structure factors for [Zn(*N*-Ph-TPP)Cl] (57 pages). Ordering information is given on any current masthead page.

Structural Diversity in Bis(pentamethylcyclopentadienyl)lanthanide Halide Complexes: X-ray Crystal Structures of $[(C_5Me_5)_2SmCl]_3$ and $(C_5Me_5)_{10}Sm_5Cl_5[Me(OCH_2CH_2)_4OMe]$

William J. Evans,*[1a,b] Donald K. Drummond,[1a] Jay W. Grate,[1a] Hongming Zhang,[1b] and Jerry L. Atwood*[1b]

Contribution from the Departments of Chemistry, University of California, Irvine, Irvine, California 92717, and University of Alabama, University, Alabama 35486.
Received November 19, 1986

Abstract: $(C_5Me_5)_2SmCl$ (THF) can be desolvated at 150 °C to form a material which crystallizes from hexane/toluene as the cyclic trimer $[(C_5Me_5)_2Sm(\mu\text{-}Cl)]_3$ in space group $C2/c$ with a = 21.665 (10) Å, b = 14.203 (8) Å, c = 20.234 (8) Å, β = 108.63 (6)°, V = 5900 Å^3, and D_{calcd} = 1.54 g cm^{-3} for Z = 4 (four trimetallic units per unit cell). The three bridging chloride ions connect the three $(C_5Me_5)_2Sm$ units via 2.849 (7)-2.892 (7) Å Sm-(μ-Cl) distances in a planar six-membered $Sm_3(\mu\text{-}Cl)_3$ ring. In the presence of tetraglyme, crystals of $\{(C_5Me_5)_2ClSm(\mu\text{-}Cl)Sm(C_5Me_5)_2[\mu,\eta^4\text{-}CH_3(OCH_2CH_2)_4OCH_3]Sm(C_5Me_5)_2\}^+\{[(C_5Me_5)_2ClSm]_2(\mu\text{-}Cl)\}^-$ form in space group $P2_1/a$ with a = 19.185 (8) Å, b = 26.627 (9) Å, c = 24.760 (9) Å, β = 115.16 (5)°, V = 11 448.3 Å^3, and D_{calcd} = 1.45 g cm^{-3} for Z = 4 (four pentametallic units per unit cell). The structure contains four independent types of $(C_5Me_5)_2Sm$ units and a variety of Sm-Cl bonds. This allows a detailed analysis of trends in structural preferences, bond distances, and angles.

Recent studies of the chemistry of organolanthanide alkyl and hydride complexes have shown that reactivity can be highly dependent on the structure of the complex.[2-7] Hence, the degree of steric saturation around the metal, the presence of terminal vs. bridging ligands, and the degree of oligomerization of the complex can strongly influence how a Ln-CR_3 or Ln-H unit reacts (Ln = lanthanide metal).[2] As a consequence, defining the

(1) (a) University of California, Irvine. (b) Alfred P. Sloan Research Fellow. (c) University of Alabama.
(2) Evans, W. J. *Adv. Organomet. Chem.* **1985**, *24*, 131-177.
(3) Schumann, H. *Angew. Chem., Int. Ed. Engl.* **1984**, *23*, 474-493.
(4) Watson, P. L.; Parshall, G. W. *Acc. Chem. Res.* **1985**, *18*, 51-56 and references therein.
(5) Evans, W. J.; Dominguez, R.; Hanusa, T. P. *Organometallics* **1986**, *5*, 263-270.
(6) Wayda, A. L.; Rogers, R. D. *Organometallics* **1985**, *4*, 1440-1444.
(7) Jeske, G.; Lauke, H.; Mauermann, H.; Schumann, H.; Marks, T. J. *J. Am. Chem. Soc.* **1985**, *107*, 8111-8118 and references therein.

0002-7863/87/1509-3928$01.50/0